Physical modelling of soil-pipe interaction for buried pipelines subjected to cyclic surface loading and internal pressurization

A. Ajami*, F. Emeriault, C. Dano, O. Jenck
Université Grenoble Alpes, CNRS, Grenoble INP, 3SR, Grenoble, France, ali.ajami@3sr-grenoble.fr

M. Polo, M. Nait Ali, G. Nespoulous
Natran, Bois-Colombes, France

ABSTRACT: Pipelines, by transporting liquid and gas, play a vital role as critical lifelines in modern infrastructure. Typically, these pipelines buried underground experience substantial stresses resulting from external cyclic loading such as traffic and soil movements, and internal pressures from conveyed fluids, including their variations over time, that have a significant influence on the structural response and long-term performance of buried pipelines. A small-scale laboratory model has been developed to study the soil-pipe interaction under these combined conditions. The experimental set-up consists of a rigid tank filled with sand, containing aluminium pipes (100 mm diameter, 2 mm wall thickness) scaled to one-third of real steel pipelines. Internal pressurization of the water-filled pipe is achieved using a Controlled Pressure Volume device, allowing the internal pressure to reach 2 MPa during testing. Surface loading with up to 1000 cycles is applied using a vertical actuator acting on a rigid plate. The instrumentation includes strain gauges on the pipe and settlement sensors on the pipe and plate. The test campaign evaluates how internal pressure influences pipe deformation and surrounding soil stress distribution under cyclic surface loading. The small-scale results obtained for both pressurized and non-pressurized cases are compared to provide a better understanding of the system behaviour. This comparison helps identify potential sources of conservatism in current design practice and highlights the importance of accounting for internal pressurization and soil–pipe interaction.

1 INTRODUCTION

One of the most complex interaction problems in geotechnical engineering is the behaviour of pipes embedded in the soil. During service, pipelines experience external cyclic loading, such as repeated traffic or ground movement, together with internal pressure variations related to operational demands. The combined effect of these actions influences pipe deformation, stability and long-term durability.

The understanding of how buried pipes respond to surrounding soil has its foundations in the early studies of Marston & Anderson (1913) for rigid pipelines and Spangler & Shafer (1938) for more flexible systems. These works highlighted that evaluating the stresses acting on a pipe cannot be separated from the behaviour of the soil that surrounds it. Since then, advances in design approaches have focused on improving how earth pressures are characterized. For example, Scarino (2003) emphasized the importance of accurately defining horizontal soil pressures, while Tian et al. (2015) proposed a parabolic representation of vertical loading to better reflect actual soil–pipe interaction conditions.

Although most laboratory and field investigations have examined buried pipelines under non-pressurized conditions (critical configuration relatively to pipe ovalisation), some studies have demonstrated that internal pressure can play a major role in defining pipeline behaviour. Robert et al. (2016) proposed a stress prediction approach that accounts for both internal pressure and external loads, demonstrating that pressurization can significantly influence the magnitude and distribution of stresses in buried pipelines.

Some of these advances have already been incorporated into practical engineering tools. For example, Natran, a French gas transmission operator, has developed the in-house design software RAMCES, which is used to estimate stress levels and deformation in buried pipelines and to assess whether additional loads can be safely tolerated. This study compares the pressurized pipe tests with the non-pressurized tests, which follow the protocol of Mertz et al. (2025). The analysis focuses on the surface settlement generated by the applied loading, the deformation of the pipe and the stresses that develop in the soil above it. This comparison provides a clear basis for evaluating the influence of internal pressurization on soil–pipe interaction.

2 MATERIAL AND METHODS

The experimental procedure aims to examine the influence of internal pressure on the response of a buried pipeline subjected to repeated surface loading. The study concentrates on the combined effect of hoop stress in the pipe from internal pressurization and vertical cyclic loading transmitted through the overlying soil.

2.1 Test tank

The experiment takes place inside a rigid steel tank with internal dimensions of 2 m × 0.8 m × 0.9 m^3. The tank walls remain fully braced to prevent lateral deformation during loading, allowing the soil–pipe interaction to develop freely within the central zone of the tank.

A vertical loading jack placed on the top frame of the tank (Figure 1) applies force through a rigid 100 × 100 mm^2 square loading plate positioned on the soil surface directly above the pipe. The system provides controlled cyclic loading with adjustable amplitude and frequency, ensuring repeatability across test conditions.

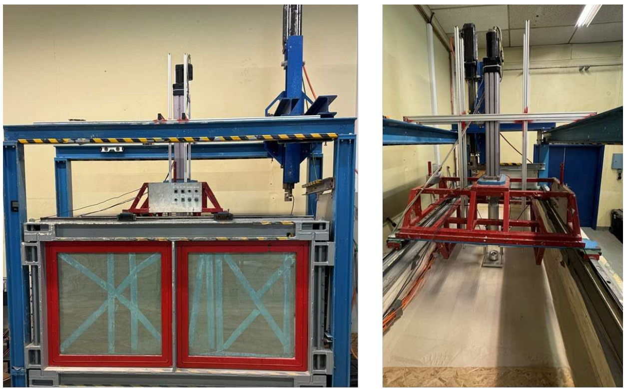

(a) (b)

Figure 1: (a) View of the test tank (b) View of the loading system above the sand-filled tank.

The soil placed in the tank consists of a siliceous sand with uniform grain size distribution and negligible fines content whose main properties are given in Table 1 (from Andria-Ntoanina et al. (2010). The sand corresponds to Fontainebleau NE34, which is widely adopted in geotechnical model testing due to its reproducibility under controlled placement procedures.

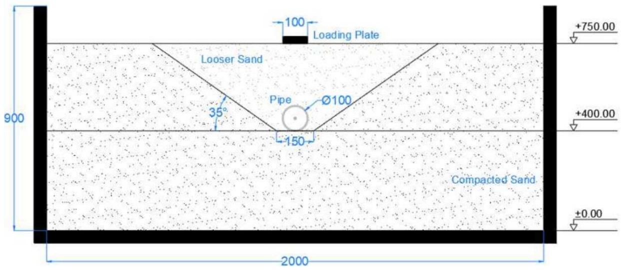

Figure 2: Schematic cross-section of the experimental setup showing the geometry, pipe location and sand layers (dimensions in mm)

Filling is done by multiple layers according to the protocol proposed by Mertz (2023), three layers of 0.2 m and one of 0.15 m, for a total sand thickness of 0.75 m. Compaction is achieved for each layer using a vibrating plate, reaching a relative density of around 72 %. The pipe is then installed by excavating a central trench within the sand bed, placing the pipe in the desired location (pipe centre being 30 cm deep), and subsequently backfilling and compacting the sand around it.

Table 1:Physical and mechanical properties of Fontainebleau sand NE34(Andria-Ntoanina. et al.,2010).

d_{50} (mm)	C_u	ρ_s (g/cm^3)	e_{min}	e_{max}	φ_{peak}	φ_{crit}
0.206	1.49	2.65	0.51	0.88	37	28

It is generally not possible in small scale experiments under normal gravity to use a model material that fully satisfies all similitude requirements for granular media; it is therefore acknowledged that the results obtained at the model scale should not be directly converted at the prototype scale. In the present case, (Mertz, 2023) has proposed to apply some empirical correction factors. For sands, it originates from the deformation modulus that depends nonlinearly on the effective stress level and can be expressed as $E \propto \sigma'^m$, where σ' is a representative effective stress (e.g., mean effective stress) and $m \in [0.5, 1]$ characterizes the stress dependency.

2.2 Pipes

Natran uses buried steel pipelines in full-scale systems, typically with diameters between 300 mm and 1200 mm and wall thicknesses of 3 mm to 30 mm. Pipes of this size and stiffness create significant constraints in laboratory testing: high self-weight, difficult handling and loading requirements that exceed the capacity of standard laboratory equipment.

To reproduce the structural behaviour of these pipelines under controlled laboratory conditions, the model follows the Vashy–Buckingham similitude approach, which links the prototype and the reduced-scale model through dimensionless parameters. By selecting a geometric scale factor (Garnier et al., 2007) of $\lambda = \frac{1}{3}$, all linear dimensions reduce by three, while stiffness-related quantities scale according to the corresponding powers of this ratio. Under this framework, the elastic modulus of the model pipe material must also align with the reduced geometry to maintain comparable bending and ovalisation stiffness relative to the surrounding soil.

Dimensional analysis gives the scale factor on other metrics of the model, such as the stresses, that should also be 1/3 of the one of prototype pipes. This also runs for the Young‘s modulus. Thus, because prototype pipe are made of steel TUE360, with a Young‘s modulus of 210 MPa, the model pipes will then be made of aluminium 6060, with a Young‘s modulus of 69.5 MPa. A use of 2 mm thickness pipe provides the most appropriate stiffness level for observing soil–pipe interaction under internal pressure and cyclic surface loading.

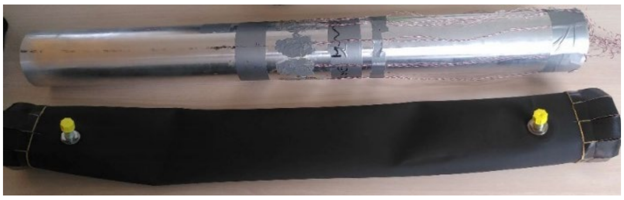

Figure 3: Photo of the aluminium pipe and internal pressurisation membrane

A flexible internal membrane is installed inside the pipe (Figure 3) to apply and maintain internal pressure. The membrane is filled with water and expands uniformly, allowing the internal pressure to increase gradually up to the target value during testing. This configuration ensures that the hoop stress state generated inside the pipe reflects that of a pressurized transmission pipeline in service. The membrane system also provides continuous pressure monitoring, since the water volume and pressure can be controlled directly through the pressurization device. The use of water instead of gas is selected for safety reasons, as pressurized gas introduces risks of rapid decompression and sudden failure in the laboratory environment.

2.3 Loading system

The loading system consists of the loading frame, the electric jack, the loading plate and the control unit. The upper part of the loading frame is equipped with a translation carriage on which is mounted an EXLAR IX-40 jack of 450 mm stroke and maximum capacity of 18.5 kN, allowing loading speeds between 0.017 mm/s and 12.7 mm/s. The loading was applied vertically at the center of the aluminium square loading plate (area: 10 × 10 cm², thickness: 2.5 cm, mass: 0.744 kg), placed at the surface of the sand mass, using the electric jack system.

The displacements of the rigid aluminium plate are monitored with four LVDT sensors, measuring the settlement and the tilting of the plate. Loading was applied with a constant velocity of the jack (0.05 mm/s) until the average stress under the loading plate reaches 100 kPa in model configuration (300 kPa at the prototype scale), with unloading/reloading loops every time the loading exceeds the previous maximum by 25 kPa. Preliminary tests showed that the bearing capacity of the soil with this surface plate geometry was reached for an average stress of around 110 kPa.

2.4 Instrumentations

To understand the behaviour of the different elements, several types of sensors are used during the experiments.

2.4.1 Strain gauges

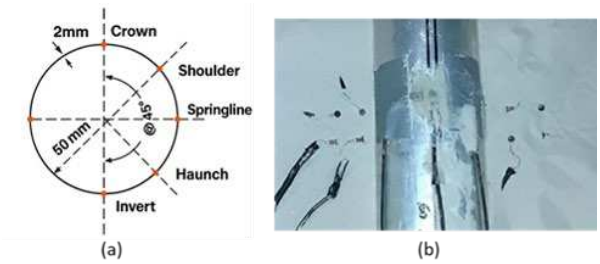

Figure 4: Placement of (a) strain gauges (b) stress sensors

To measure the deformations and then deduce the stresses acting on the pipe in both longitudinal and ortho-radial (hoop) directions, 6 bi-directional strain gauges were used. The gauges were placed at the outer surface of the pipe in 6 different positions (crown, shoulder, both sides of springline, haunch and invert) in the central part (i.e., 45.5 cm from the edge of the pipe) as shown in Figure 4(a).

2.4.2 Stress sensors

To investigate the evolution of the stresses into the soil, around the pipe, 10 pairs of vertical and horizontal miniature stress sensors of 200 kPa capacity (diameter D_{sensor} = 6mm and thickness t_{sensor} = 0.6mm) were placed at 8 different places in the sand during the tests.

At the lateral sides of the pipe, 2 paired sensors (one horizontal and one vertical at each side) capture the stress redistribution along the springline region (Figure 4(b)). 3 vertical sensors are positioned below the pipe to follow stress concentration and load transfer toward the invert. 5 vertical sensors are positioned above the pipe, forming a vertical stress profile between the pipe crown and the ground surface. All sensors are placed at a radial offset of 2.5 cm from the pipe surface, and the spacing between neighboring sensors also remains 2.5 cm, ensuring independent stress readings without mutual interference. This spatial layout provides a detailed stress field map around the pipe during both the application of internal pressure and cyclic surface loading.

2.4.3 CPV system

Internal pressurization of the pipeline is controlled using a Controlled Pressure–Volume (CPV) device (Figure 5). The system includes a hydraulic cylinder, a piston and a digital control unit that regulates the injected water volume and the resulting internal pressure inside the pipe. The CPV connects to the membrane-lined pipe through a sealed tube, allowing water circulation and stable pressure adjustment during each loading stage. The device records pressure and injected volume continuously, ensuring precise control during pressurization and unloading cycles.

Figure 5: Picture of the controlled pressure-volume (CPV) connected to the pipe system

In Natran transmission networks, pipelines typically transport gas at pressures close to 6 MPa. To reproduce the mechanical state of the prototype pipeline while maintaining safe testing conditions, the internal pressure level scales according to the 1/3 geometric similarity applied to the pipeline model. Under this scaling, the equivalent internal pressure in the reduced model corresponds to approximately 2 MPa, which the CPV system maintains accurately and safely.

2.5 Experimental procedure

According to the protocol established by Mertz (2023), each test follows a defined construction and preparation sequence. The procedure begins with reopening the trench and removing the pipe and all sensors. The protocol then requires complete backfilling of the trench and compaction with a vibrating plate. After this stage, the procedure calls for opening the trench again at a 35° angle, as described earlier. The protocol then defines the placement of the pipe and the installation of the sensors while adding backfill in successive 2.5-cm layers. Two final layers of 20 cm and 15 cm complete the backfilling, and the loading phase follows. This procedure also applies to the non-pressurized condition and to the reference case where no pipe is present.

In the new pressurized configuration, the protocol retains the same sequence up to sand filling completed. After filling the tank, the procedure introduces internal pressure in the pipe in two stages. Tap water first fills the pipe and raises the internal pressure to 500 kPa. After reaching this level, the protocol connects a compact CPV hydraulic pressure intensifier through a 2-m flexible tube and establishes uniform internal pressure inside the pipe, consistent with the conditions of the experimental tank. The CPV system then increases the internal pressure gradually from 500 kPa to 2 MPa with precise control. After reaching the target pressure, the procedure sets all strain gauges to zero to record only the deformation generated by the external loading.

3 RESULTS

3.1 Average stress on the surface plate vs average settlement of the plate

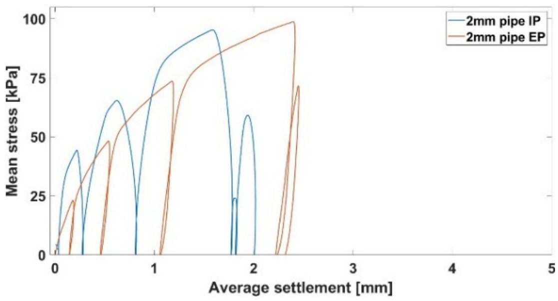

Figure 6: Average stress curve - average settlement for tests with internal pressure (IP) and without internal pressure (EP) within the pipe

The stress–settlement curves measured after backfilling as shown in Figure 6, reveal a behaviour that is broadly similar between the two configurations containing pipes, but with a few noticeable differences. Despite these differences, the two tests remain consistent in the overall shape of their stress–settlement response. The key distinction lies in the amplitude of settlement reached at equivalent stress levels showing a stiffer response for the pipe IP test (Including Pressure) test and a marginally softer global response, for the pipe EP test (Excluding Pressure) throughout loading. Such variations observed between the two tests may be linked either to the compaction or to the presence of internal pressure in the tube, which can influence the deformation response. To clearly distinguish the influence of these factors, an additional repeatability test would be required to obtain a more accurate and reliable assessment.

3.2 Stress distribution in the pipe after pressurization

In a thin-walled pressure vessel, where the wall thickness t = 2 mm is much smaller than the pipe radius r = 50 mm (t/r < 0.1), the stress distribution across the wall thickness remains approximately uniform. Under internal pressure, the pipe develops two principal membrane stresses: the hoop (circumferential) stress $\sigma_{\theta\theta}$ acting around the circumference and the longitudinal stress σ_{zz} acting along the pipe axis (Ibrahim et al., 2015). For an internal pressure of 2 MPa, the thin-wall formulas give $\sigma_{\theta\theta} \approx 50$ MPa and $\sigma_{zz} \approx 25$ MPa.

$$\sigma_{\theta\theta} = \frac{p.r}{t} \tag{1}$$

$$\sigma_{zz} = \frac{p.r}{2t} \tag{2}$$

where p (kPa) is the internal pressure, r (mm) is the average radius of the pipe, t (mm) is the thickness of the pipe.

The ortho-radial strain of approximately 500 με measured during the pressurization phase agrees with the expected elastic response associated with the hoop stress. After zeroing the strain gauges at 2 MPa full pressurization, the elastic hoop strain associated with the internal pressure (≈500 με) remains part of the actual strain state and must therefore be included in the final strain evaluation.

3.3 Pipe deformation at first surface loading

Figure 7 and Figure 8 present the ortho-radial and longitudinal deformations respectively recorded by strain gauges positioned at different angular locations around the pipe under a 100 kPa surface mean stress, at first surface loading. Two loading conditions appear, IP (Including Pressure), where the pipe contained 2 MPa internal pressure, and EP (Excluding Pressure), where the pipe experienced only the external load. In both conditions, the strain gauges showed zero values immediately after pressurization, due to the zeroing procedure, so the recorded values represent deformation only due to the applied surface load.

For the orthoradial deformation shown in Figure 7, both the internal pressure (IP) and external pressure (EP) conditions exhibit very similar deformation behaviour and an almost identical circumferential distribution, with overall differences between IP and EP remaining within approximately 5%. This indicates that the deformation pattern induced by external loading is largely preserved after the application of internal pressure.

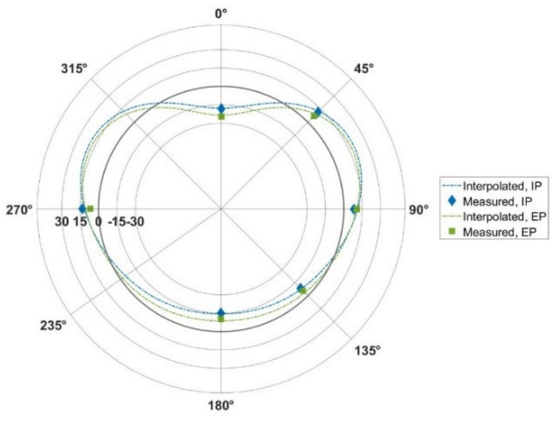

Figure 7: Ortho-radial deformation [µdef] for pipe at 100 kPa surface loading for IP and EP

At the crown (0°), both IP and EP conditions show compressive deformation due to the vertical external load acting on the pipe. The compression under IP is slightly reduced compared to EP. Between 45° and 90°, the deformation transitions into tension for both loading cases, reflecting stress redistribution associated with crown loading, with nearly identical trends observed. Toward the haunch region (135°), the deformation gradually shifts back toward compression, and the shapes of the IP and EP curves remain closely aligned. At the invert (180°), compressive orthoradial deformation is observed for both conditions as a result of external loading and pipe ovalisation, with IP again producing a marginally lower compressive response.

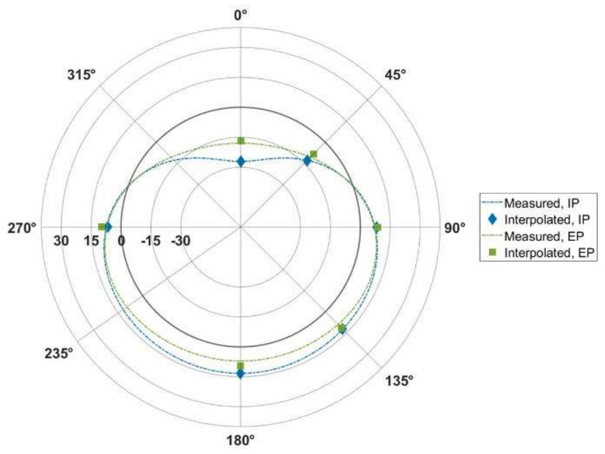

Figure 8: Longitudinal deformation [µdef] of pipe shaft at 100 kPa surface loading for IP and EP

For the longitudinal deformation shown in Figure 8, IP and EP display similar overall trends but differ locally along the circumference. Differences at 45° are negligible, whereas more pronounced discrepancies are observed at the crown and the invert, where EP pipe exhibits greater compression and tension, respectively, compared to IP pipe.

3.4 Pipe deformation under surface cyclic loading

When comparing the deformation patterns obtained without pressure (Figure 9 and Figure 11) to those measured with internal pressure (Figure 10 and Figure 12), the overall behaviour of the pipe remains stable under cyclic loading, but some local differences appear once pressure is introduced.

In ortho-radial direction, the test without pressure (Figure 9) shows almost no evolution throughout the 1000 cycles, with very small variations mainly near the invert and a deformation field that stays nearly symmetric. In the test with internal pressure (Figure 10), the general shape is still preserved and the deformation remains stable at 45° and 180°, but two regions show a more noticeable evolution. An increase in deformation appears near 90° and 270° after 1000 cycles, where the curves diverge more than in the no-pressure case. The reading at 0° shows mainly the effect of internal pressure over time to rearrange the effect of the loading where the compression value decreased from -20 µdef reaching -5 µdef after 1000 cycle. Overall, internal pressure seems to enhance localized variations, while the global ortho-radial behaviour remains controlled.

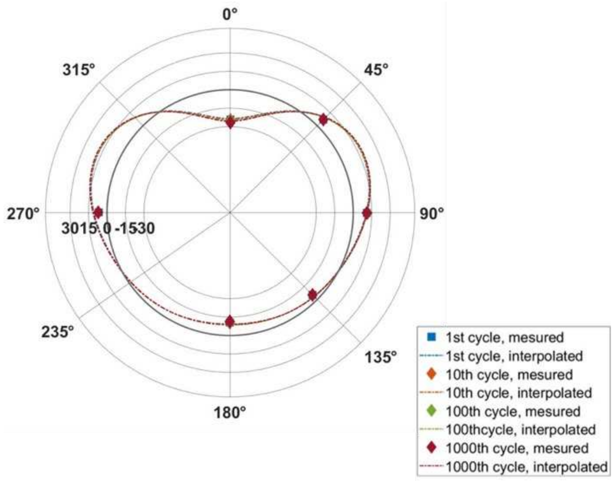

Figure 9: Ortho-radial deformations [µdef] of pipe shaft at 100 kPa surface loading, without pressure (EP), under cyclic loading

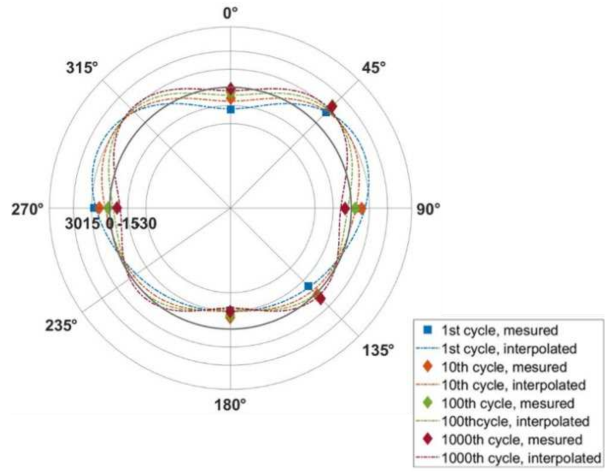

Figure 10: Ortho-radial deformations [µdef] at 100 kPa surface loading, with pressure (IP), under cyclic loading

In Figure 11, the longitudinal deformation shows only limited evolution, with the largest variations occurring near the crown but remaining small in amplitude. In the test with pressure (Figure 12), the deformation curves do not superimpose from one cycle to the next. A gradual evolution of the longitudinal deformation is observed with increasing cycles, characterized by a localized increase near 0°, while the rest of the circumference exhibits only minor changes. Although the overall deformation level remains low, the presence of pressure induces a slight but persistent modification of the longitudinal deformation distribution compared with the no-pressure case.

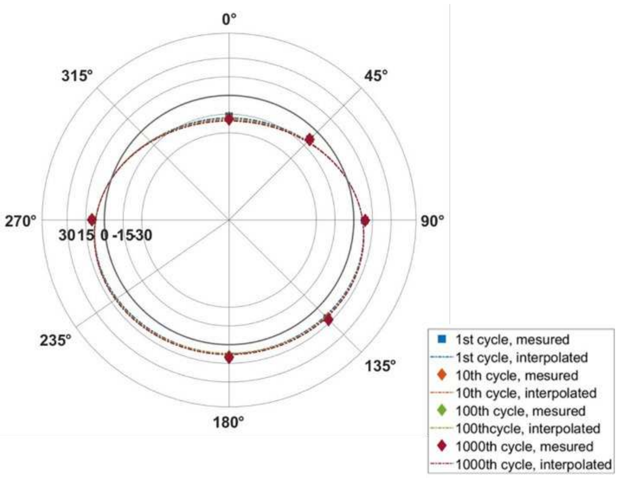

Figure 11: Longitudinal deformations [µdef] at 100 kPa surface loading without pressure (EP), under cyclic loading

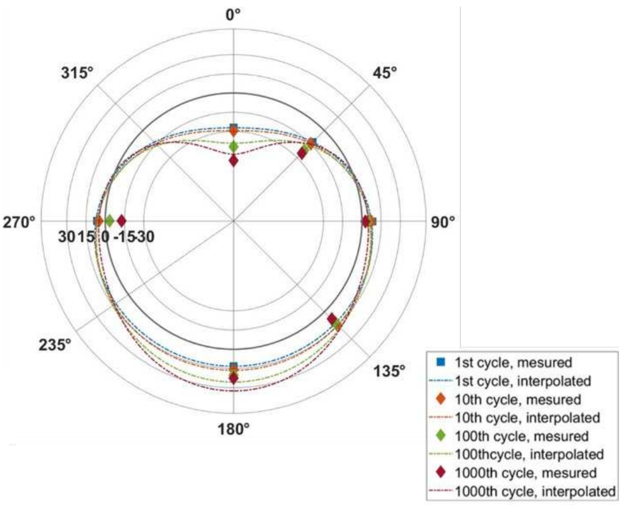

Figure 12: Longitudinal deformations [µdef] at 100 kPa surface loading with pressure (IP), under cyclic loading

3.5 Stress in the soil above the pipe

The vertical stresses presented in Figure 13 correspond to the incremental vertical stress induced by the applied surface loading. The sensors were zeroed at the start of the loading sequence, so the curves do not include the initial soil stresses from burial and compaction. The reported values represent the stress state after the completion of the 1000 loading cycles under a surface loading of 100 kPa. The results show that the vertical stress directly above the pipe is noticeably lower compared to the surrounding soil. The minimum stress occurs at the pipe crown (0°), measuring approximately 16.6 kPa, while the stress increases progressively moving away from the centre, reaching approximately 23.7 kPa at −2.5 cm and 24.2 kPa at −5 cm, and 18.4 kPa at +2.5 cm and 20.0 kPa at +5 cm. Overall, the incremental stress at the edges is roughly 20–30% higher than the stress measured directly above the pipe.

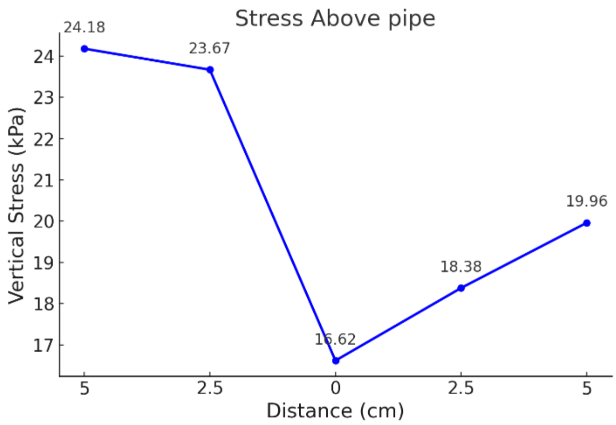

Figure 13: Incremental vertical stress above pipe after cyclic loading, for IP test.

This non-uniform stress distribution suggests the developement of soil arching, where the load is being transferred away from the pipe. Further analysis is required, in particular comparison with arching theories such as developed by Marston & Anderson (1913) or Spangler & Schafer (1938) as well repeatability experiments in which all the stress sensors would be efficient and additional tests without inner pressure to queantify its effect on the observed arching phenomenon..

4 CONCLUSION

The physical modelling results indicate that internal pipe pressure increases hoop stiffness (reduction of circumferential deformation) under surface loading. The vertical stress measurements indicate arching effect above the pipe, with reduced stress at the crown and higher stresses toward the pipe shoulders. These findings highlight the importance of accounting for internal pressure when evaluating buried pipeline performance under operational loading.

This work will be extended by introducing a numerical model capable of assessing parameters that cannot be directly captured in the laboratory, providing a more complete characterization of soil–pipe interaction behaviour.

ACKNOWLEDGEMENTS

The authors would like to acknowledge Grenoble Civil Engineering Department at IUT for providing the research facilities and institutional support necessary to conduct this study.

REFERENCES

Andria-Ntoanina., I., Canou, J., & Dupla, J.-C. (2010). *Mechanical characterization of Fontainebleau NE34 sand with monotonic triaxial test.* France: CERMES, ENPC/LCPC.

Dano, C. (2001). *Mechanical behavior of injected soils (in french).* PhD thesis, Ecole Centrale Nantes.

Garnier, J., Gaudin, C., Springman, S.M., Culligan, P.J., Goodings, D., Konig, D., Kutter, B., Phillips, R., Randolph, M.F., & Thorel, L. (2007). Catalogue of scaling laws and similitude questions in geotechnical centrifuge modelling. *International Journal of Physical Modelling in Geotechnics,* *7*(3), 1-23. doi:10.1680/ijpmg.2007.070301

Ibrahim, A., Ryu, Y., & Saidpou, M. (2015). Stress Analysis of Thin-Walled Pressure. *Modern Mechanical Engineering,* *5*(1), 1-9. doi:10.4236/mme.2015.51001

Marston, A., & Anderson, O. (1913). *The theory of loads on pipes in ditches.* Iowa, USA: Iowa Engineering Experiment Station.

Mertz, A. (2023). *Behavior of model buried gas pipelines under patch surface loading (in french).* PhD thesis, Université Grenoble Alpes.

Mertz, A., Ajami, A., Dano, C., Emeriault, F., Jenck, O., Fernandez, C., Lebrun, A., & Polo, M. (2025). Mechanical behaviour of model gas pipes buried into sand and loaded in surface. *International Journal of Physical Modelling in Geotechnics, 25*, 1-20. doi:10.1680/jphmg.24.00056

Robert, D. J., Rajeev, P., Kodikara, J., & Rajani, B. (2016). Equation to predict maximum pipe stress incorporating internal and external loadings on buried pipes. *Canadian Geotechnical Journal,* *53*(8), 1315-1331. doi:10.1139/cgj-2015-0142

Scarino, H. (2003). Reappraisal of Marston's Formula. *Journal of Transportation Engineering,* *129*(6), 703-712. doi:10.1061/(ASCE)0733-947X(2003)129:6(703)

Spangler, M., & Shafer, G. (1938). The structural design of flexible pipe culverts. *Highway Research Board Proceedings* (pp. 235-239). USA: 17.

Tian, Y., Liu, H., Jiang, X., & Yu, R. (2015). Analysis of stress and deformation of a positive buried pipe using the improved Spangler model. *Soils and Foundations,* *55*(3), 485-492. doi:10.1016/j.sandf.2015.04.001

Wu, J. T.-Y. (2019). Determination of Model Parameters for the Hardening Soil Model. *Transportation Infrastructure Geotechnology*.